MOLECULAR AND CELLULAR BIOLOGY, May 2011, p. 1822–1832 Vol. 31, No. 9
0270-7306/11/$12.00 doi:10.1128/MCB.01026-10

Elongator Protein 3b Negatively Regulates Ribosomal DNA Transcription in African Trypanosomes▽†

Sam Alsford and David Horn*

London School of Hygiene and Tropical Medicine, Keppel Street, London WC1E 7HT, United Kingdom

Received 1 September 2010/Returned for modification 28 September 2010/Accepted 16 February 2011

Eukaryotic cells limit ribosomal DNA (rDNA) transcription by RNA polymerase I (RNAP-I) to maintain genome integrity. African trypanosomes present an excellent model for studies on RNAP-I regulation because they possess a bifunctional RNAP-I and because RNAP-II transcription appears unregulated. Since Elp3, the catalytic component of Elongator, controls RNAP-II transcription in yeast and human cells, we predicted a role for a trypanosome Elp3-related protein, ELP3a or ELP3b, in RNAP-I regulation. *elp3b* null and conditional strains specifically exhibited resistance to a transcription elongation inhibitor, suggesting that ELP3b negatively impacts elongation. Nascent RNA analysis and expression of integrated reporter cassettes supported this interpretation and revealed negative control of rDNA transcription. ELP3b specifically localized to the nucleolus, and ELP3b loss rendered cells hypersensitive to DNA damage and to translation inhibition, suggesting that anti-Elongator function was important to maintain genome integrity rather than to modulate ribosome production. Finally, ELP3b displayed discrimination between RNAP-I compartments in the same cell. Our results establish ELP3b as a major negative regulator of rDNA transcription and extend the roles of the Elp3-related proteins to RNAP-I transcription units. ELP3b is also the first trypanosome protein shown to distinguish between rDNA and variant surface glycoprotein transcription within different RNAP-I compartments.

In eukaryotic cells, RNA polymerase II (RNAP-II) transcription regulation appears to operate predominantly at the level of elongation (18), and several factors that influence this process have been described in human cells and in model organisms (43). Much less is known about RNAP-I control, but cells do limit ribosomal DNA (rDNA) transcription, and this is important for the maintenance of genome integrity (22); extra copies of rDNA allow for reduced transcription, which facilitates repair.

Trypanosomatids are protozoa that branched early from the eukaryotic lineage and are important human and animal pathogens which are emerging as model organisms for the study of epigenetic regulation (13). In trypanosomatids, RNAP-II transcription of protein-coding genes is polycistronic and apparently constitutive (10). In the bloodstream-form African trypanosome *Trypanosoma brucei*, RNAP-I is bifunctional, directing transcription of rDNA in the nucleolus and monotelomeric transcription of a variant surface glycoprotein (*VSG*) gene in an expression site body (ESB) that is distinct from the nucleolus (32). RNAP-I is readily able to contribute to mRNA production in trypanosomatids (45) because all mature mRNAs are fused to an RNAP-II-transcribed, *trans*-spliced leader sequence (19). The high rate of transcription achieved by RNAP-I may be important for *VSG* expression since *T. brucei* bloodstream-form cells derive >10% of total cellular protein from a single *VSG* gene. These features lead us to predict that conserved factors involved in RNAP-II transcription elongation control in other eukaryotes, such as Elongator, might function in RNAP-I control in trypanosomes.

Saccharomyces cerevisiae Elongator (49) associates with elongating RNA polymerase II (RNAP-II) with a hyperphosphorylated carboxyl-terminal domain (37). The catalytic subunit of the six-subunit Elongator complex (26), Elp3 (Elongator protein 3, also called KAT9), appears to provide a direct link between histone acetylation and transcription by facilitating RNAP-II elongation in a chromatin- and acetyl coenzyme A (acetyl-CoA)-dependent manner (56, 57). Human Elongator also facilitates RNAP-II elongation through chromatin and displays histone acetyltransferase activity with specificity for lysine residues in the N-terminal tail of histone H3 (25). More recently, *S. cerevisiae* Elp3 was shown to modulate transcriptional silencing at telomeres and to modulate DNA repair through an interaction with proliferating cell nuclear antigen (28). As well as a GNAT-type acetyltransferase domain, Elp3 contains a radical *S*-adenosylmethionine (SAM) domain with an iron-sulfur (FeS) cluster. Recent evidence points to a role for the mouse Elp3 radical SAM domain in DNA demethylation (36). Surprisingly, *S. cerevisiae* Elongator (40, 41) and human Elongator (25) localize predominantly to the cytoplasm, and roles have also been reported in exocytosis (41) and tRNA metabolism in *S. cerevisiae* (21) and in tubulin acetylation in mouse neurons (11).

There are two Elp3-related proteins in trypanosomatids, and we predicted a role for one or both of these proteins in RNAP-I regulation. Here, we demonstrate that *T. brucei* ELP3b negatively regulates rDNA transcription. This conclusion is supported by elongation inhibitor resistance, increased nascent rDNA transcription, and increased rDNA-integrated

* Corresponding author. Mailing address: London School of Hygiene and Tropical Medicine, Keppel Street, London WC1E 7HT, United Kingdom. Phone: (44) 20 7927 2352. Fax: (44) 20 7636 8739. E-mail: david.horn@lshtm.ac.uk.

▽ Published ahead of print on 28 February 2011.

† The authors have paid a fee to allow immediate free access to this article.

reporter expression in *elp3b*-depleted strains and ELP3b nucleolar localization. Remarkably, ELP3b selectively controls rDNA transcription, indicating an ability to distinguish between different RNAP-I transcription units.

MATERIALS AND METHODS

Trypanosomes. Bloodstream forms of *T. brucei*, MiTat 1.2 clone 221a, were maintained, transfected, and differentiated as previously described (3). At least 5 h after transfection, transformants were exposed to puromycin (2 μg ml^{-1}; phosphonoacetic acid [PAA]), blasticidin (10 μg ml^{-1}), hygromycin (2.5 μg ml^{-1}), or phleomycin (2 μg ml^{-1}) selection, as appropriate. *ELP3b* disruption was confirmed by PCR and Southern blotting, using standard protocols (5). For conditional strains, pHD1313 (Tet-R) (1), was integrated at the β-tubulin locus and pRP^{iGFP}ELP3b was integrated at an rDNA locus in an *ELP3b* heterozygous strain prior to disruption of the second native allele of *ELP3b*. Transformants were screened by immunoblotting and immunofluorescence to confirm robust regulated expression, and two strains were transformed with the final disruption construct in the presence of tetracycline (Tet; 1 μg ml^{-1}) to generate four conditional strains. For growth assays, cultures were seeded at ~10^5 ml^{-1} and diluted back every 24 h. Cell counts were made using a hemocytometer and carried out over at least 72 h. Cumulative counts were used to calculate population doubling times, assuming exponential growth. For half-maximal effective concentration (EC_{50}) determinations, cells were seeded at 2 × 10^3 ml^{-1} in 96-well plates in a 2-fold dilution series of drug. After ~3 days of growth, 20 μl of Alamar blue (AbD Serotec) was added to each well, and the plates were incubated for a further 7 h. Fluorescence was determined using a fluorescence plate reader (Molecular Devices) at an excitation wavelength of 530 nm, an emission wavelength of 585 nm, and a filter cutoff of 570 nm (42). All assays were carried out in the absence of any additional antibiotics.

Plasmid construction. Enhanced green fluorescent protein (eGFP) and cMYC fusions were generated using the pRP (*ELP3a*, *ELP3b*, *RPB6z*, and *RPB6*) and pNAT (*SNAP42* and *RPC160*) vectors (2). Protein-coding sequences were amplified from *T. brucei* genomic DNA using Phusion polymerase (New England BioLabs). Primers were designed using the publicly available *T. brucei* genome sequence (www.genedb.org/genedb/tryp/). For the generation of *ELP3b* disruption constructs, targeting fragments were amplified from genomic DNA and cloned into pBLA (blasticidin S deaminase) and pPAC (puromycin *N*-acetyltransferase). *ELP3a* targeting fragments were cloned into pPAC; the *PAC* gene was subsequently replaced with *BLE* and *HYG* to generate additional disruption constructs. All transcription run-on probes were cloned in pBluescript (Stratagene) or pGEM-T Easy (Promega) with the exception of R3, which proved refractory to cloning. All primer sequences are available upon request.

Protein analysis. Immunoblotting was carried out following SDS-PAGE of whole-cell lysates and electroblotting using standard protocols (5) and an enhanced chemiluminescence kit (Amersham), according to the manufacturer's instructions. Immunofluorescence analysis was carried out on fixed cells settled onto slides pretreated with 3-aminopropyl triethoxysilane (Sigma) and processed as previously described (4). eGFP and cMYC fusions were detected with rabbit polyclonal anti-GFP (Molecular Probes) or mouse monoclonal anti-GFP (AbCam) and mouse anti-cMYC (9E10; Santa Cruz Biotechnology), respectively. NOG1 and NUP1 were detected with rabbit anti-NOG1 (38) and mouse anti-NUP1 (35), respectively. Images were captured using a Nikon Eclipse E600 epifluorescence microscope in conjunction with a Coolsnap FX (Photometrics) charge-coupled device (CCD) camera and processed in Metamorph 5.0 (Photometrics) and Adobe Photoshop elements 2.0 (Adobe).

Transcript analysis. Total RNA was isolated using an RNeasy kit (Qiagen), fractionated on 5% polyacrylamide-7 M urea or 1.5% agarose-formaldehyde gels, and analyzed by Northern blotting according to standard protocols (5). Transcription run-on analysis was carried out using an adapted lysolecithin permeabilization protocol (51). Briefly, ~2 × 10^8 cells were washed in transcription buffer (TB; 20 mM L-glutamic acid monopotassium salt, 3 mM $MgCl_2$, 150 mM sucrose, 1 mM dithiothreitol [DTT], 10 μg ml 1-leupeptin [Sigma]) and incubated for 1 m in 0.4 ml TB containing 0.2 mg lysolecithin (L-α-lysophosphatidylcholine palmitoyl [Sigma]) on ice. Permeabilized cells were washed in TB and then placed in labeling mix (20 mM L-glutamic acid [monopotassium salt], 3 mM $MgCl_2$, 1 mM DTT, 10 μg ml^{-1} leupeptin, 25 mM creatine phosphate, 0.6 μg ml^{-1} creatine phosphokinase [type I, rabbit muscle; Sigma], 2 mM ATP, 1 mM CTP, 1 mM GTP [Fermentas], 100 μCi [α-^{32}P]UTP [Perkin-Elmer]) in a final volume of 200 μl for 15 m at 37°C. Total RNA was isolated using an RNeasy kit (Qiagen). Slot blots were generated in sets of three and included seven rDNA probes: R1 (rDNA promoter; −244 to +255), R2 (including the rDNA promoter and the first 400 bp of small-subunit [SSU] rDNA; RH6), R3 (+1 to 3310, including SSU rDNA), R4 (+3339 to 6389, including 5.8S and large-subunit α [LSUα] rDNA), R5 (+6444 to 9455, including LSUβ rDNA), R6 (nontranscribed rDNA spacer), and 5S rDNA; four mRNA-associated probes, *VSG2*, β-*tubulin*, *Procyclin*, and spliced-leader RNA (SL-RNA); and a pBluescript negative control. Three micrograms of each plasmid (or 1.5 μg of purified R3 PCR product) was denatured in 0.4 M NaOH, transferred to nylon membrane under vacuum, and UV cross-linked. Total labeled RNA was hybridized to the slot blots overnight at 65°C and subsequently washed and processed according to standard protocols (5). Hybridization signals were detected using a Typhoon phosphorimager (Amersham), quantified using ImageQuant (Amersham), and analyzed in MS Excel.

RESULTS

Trypanosomatid genomes encode two Elp3-related proteins. Elp3 orthologues are conserved from archaea to humans. Pairs of Elp3 orthologues were identified in *T. brucei*, *Trypanosoma cruzi*, and *Leishmania major* (23), but we found no organism beyond the trypanosomatids with more than one Elp3 orthologue. As expected from the position in the Excavata, the trypanosomatid Elp3 orthologues, designated ELP3a and ELP3b, are diverged relative to Elp3 orthologues from the Opisthokonta, i.e., metazoa, plants, fungi, and alveolates (Fig. 1A). In addition, the ELP3a and ELP3b paralogue groups are monophyletic, suggesting a single gene duplication that predates divergence of the trypanosomatids. Despite the divergence, the residues required for substrate binding within both the radical SAM and acetyltransferase domains are conserved in both *T. brucei* ELP3a and ELP3b (Fig. 1B). Our phylogenetic and sequence analysis indicated that ELP3a and ELP3b have similar features regardless of the trypanosomatid under consideration; we have focused on the *T. brucei* proteins.

***elp3b* mutants are resistant to transcription elongation inhibition and hypersensitive to DNA-damaging agents.** To explore the function of the trypanosomatid Elp3-related proteins, we generated *elp3a* (Fig. 2A) and *elp3b* (Fig. 2B) null strains. Double-null *elp3a*/*elp3b* strains were also generated (Fig. 2A and B). These strains were indistinguishable from wild type in relation to cell cycle phase distribution and differentiation to the insect stage (data not shown), but the *elp3b* strains displayed a growth defect relative to *elp3a* and wild-type trypanosomes (Fig. 2C). Interestingly, repeating the analysis after further growth suggested that the cells were adapting to the defect, with population doubling time approaching that of wild-type cells (Fig. 2C). Double-null *elp3a*/*elp3b* strains also displayed a growth defect and partial reversal of this phenotype after prolonged growth. Transcription elongation defects increase sensitivity to depleted nucleoside triphosphate (NTP) substrate pools. Indeed, *S. cerevisiae elp3* null strains were hypersensitive to 6-azauracil (6AU) (57), which inhibits IMP dehydrogenase (IMPDH) and depletes pools of GTP and UTP (46). Surprisingly, *elp3b* cells displayed specific and significant resistance to 6AU relative to that of *elp3a* and wild-type trypanosomes (Fig. 2D), suggesting that ELP3b negatively controls transcription elongation. This phenotype, like the growth phenotype, was diminished after further growth (Fig. 2E). Double-null *elp3a*/*elp3b* strains also displayed 6AU resistance and partial reversal of this phenotype after prolonged growth. Thus, *elp3b* null cells display an adaptation phenomenon characterized by partial reversal of the growth and 6AU resistance phenotypes, and ELP3a is not required for this adaptation.

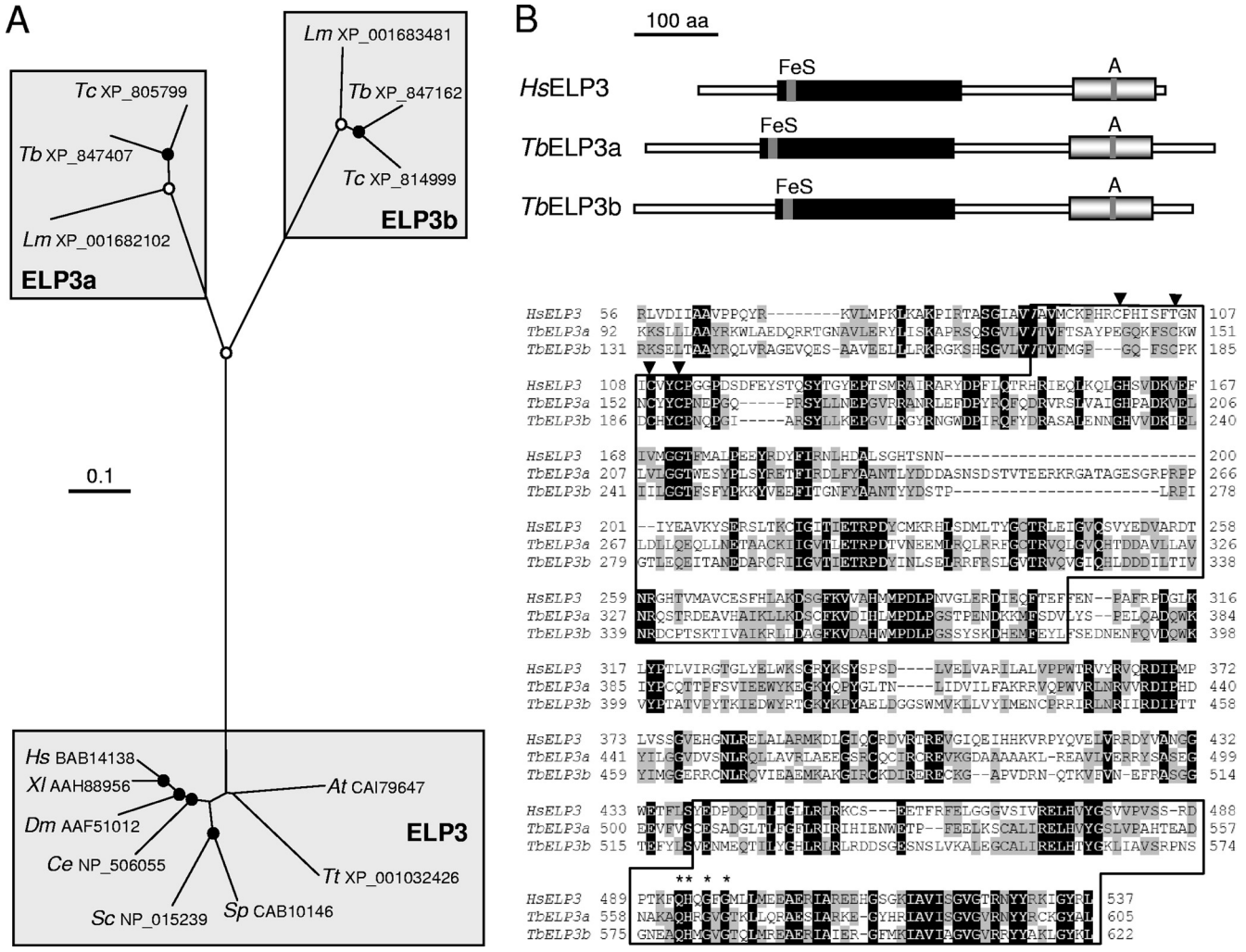

FIG. 1. Phylogenetic and sequence analysis of Elp3 orthologues. (A) ELP3a and ELP3b were identified in *T. brucei* (*Tb*), *T. cruzi* (*Tc*), and *Leishmania major* (*Lm*). The unrooted neighbor-joining tree was generated using CLUSTAL 1.8X and TreeView. Where excellent (≥99.9%, open circles) or very good (≥90%, closed circles), branching confidence is indicated. *Hs*, *Homo sapiens*; *Xl*, *Xenopus laevis*; *Dm*, *Drosophila melanogaster*; *Ce*, *Caenorhabditis elegans*; *Sc*, *Saccharomyces cerevisiae*; *Sp*, *Schizosaccharomyces pombe*; *Tt*, *Tetrahymena thermophila*; *At*, *Arabidopsis thaliana.* All accession numbers are indicated. The GeneIDs for the *T. brucei* proteins are as follows: *Tb*ELP3a, Tb927.8.5770; *Tc*ELP3a, Tc00.1047053503851.10; *Lm*ELP3a, LmjF16.0240; *Tb*ELP3b, Tb927.8.3310; *Tc*ELP3b, Tc00.1047053509769.110; *Lm*ELP3b, LmjF23.1350. (B) Schematic representation of the predicted structures of *T. brucei* ELP3a and ELP3b compared with human Elp3. The radical SAM domains (black boxes) and GNAT-type acetyltransferase domains (gray boxes) are indicated with the FeS cluster and motif A, respectively. The sequences were aligned using ClustalW, and the conserved domains (boxed) are indicated. Residues that are shared between all three proteins are white on a black background, and residues shared among any pair of proteins are on a gray background. Arrowheads indicate the Cys residues that form part of the FeS cluster. Asterisks indicate the conserved residues of motif A, QHXGXG, in all Elp3 orthologues.

The data above are consistent with the idea that ELP3b negatively controls transcription, and preliminary analysis of nascent RNA did indeed reveal increased rDNA transcription in *elp3b* cells (data not shown). Consistent with a link between the growth and 6AU resistance phenotypes described above, the rDNA transcription derepression phenotype was also unstable (data not shown but see below). *Saccharomyces cerevisiae* strains lacking Elp3 (28) or with increased rDNA transcription (22) are hypersensitive to DNA-damaging agents, and notably, *elp3b* null cells were also hypersensitive to phleomycin (Fig. 2F), an agent that damages DNA via a mechanism involving chelation of metal ions and the generation of free radicals.

To facilitate studies of ELP3b function in a controlled environment, we generated strains with a conditional (Tet-on) copy of ^{GFP}ELP3b in an *elp3b* null background. Cells in which ^{GFP}ELP3b expression was inactivated (Fig. 3A) displayed decreased growth rate (Fig. 3B), reduced 6AU sensitivity (Fig. 3C), and increased sensitivity to methyl methanesulfonate (MMS) (Fig. 3D), an alkylating agent that damages DNA and is thought to stall replication forks. These results recapitulate the *elp3b* null phenotypes and demonstrate that ^{GFP}ELP3b functionally complements the *elp3b* defect.

ELP3b negatively controls ribosomal DNA transcription elongation. We next measured nascent transcripts emanating from different loci in cells expressing ^{GFP}ELP3b or in cells

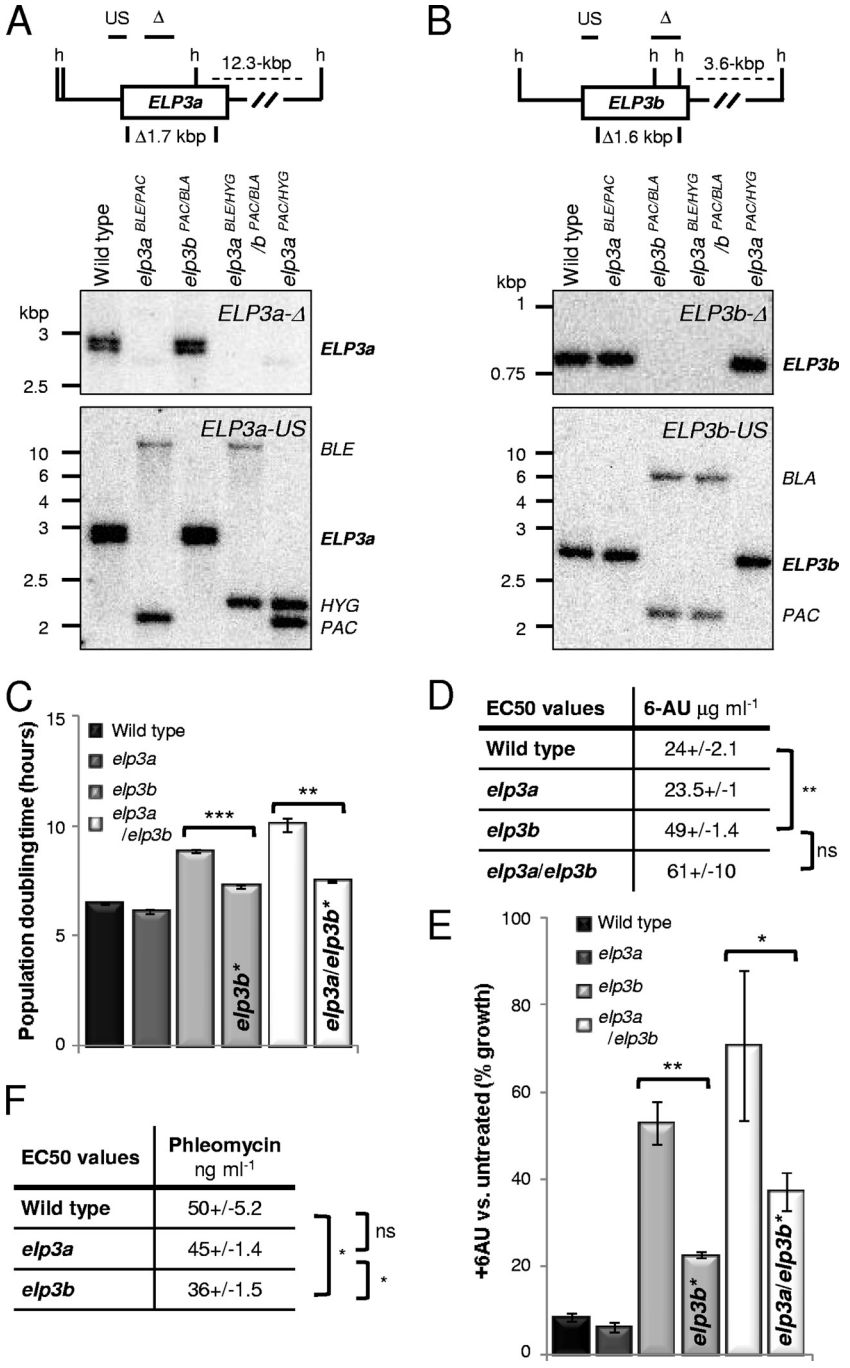

FIG. 2. ELP3b loss is associated with unstable resistance to transcription inhibition and hypersensitivity to a DNA-damaging agent. (A) Southern blot indicating ELP3a disruption. Genomic DNA was digested with HindIII. The map details the HindIII sites (h), deleted regions, and probes used (horizontal bars). The deleted region was replaced with the selectable marker *BLE*, *HYG*, or *PAC*; the *HYG* and *PAC* cassettes each contain a HindIII site. The *elp3aPAC*/*HYG* strain was used for the assay shown in panel F. (B) Southern blot indicating ELP3b disruption. The deleted region was replaced with the selectable marker *PAC* or *BLA*. Other details are as in panel A. (C) Population doubling time in wild-type strain and *elp3a*, *elp3b*, and *elp3a*/*elp3b* strains. *elp3b** and *elp3a*/*elp3b** strains were maintained in culture for more than 8 weeks. Standard deviations are indicated, and *P* values were derived using an unpaired Student *t* test. ***, $P < 0.001$; **, $P < 0.01$; *, $P < 0.05$; ns, not significant. (D) Half-maximal effective concentrations (EC_{50}) for 6AU. All data were derived from two wild-type samples and two independent null strains. Other details are as in panel C above. (E) 6AU sensitivity (50 μg ml^{-1}). Other details are as in panel C above. (F) EC_{50} for phleomycin. Other details are as in panel C above.

where ^{GFP}ELP3b expression had been inactivated for 3 or 7 days (Fig. 4). In this case, we used a series of five probes (R1 to R5) covering the length of the rDNA transcription unit (Fig. 4A). Slot blots were also loaded with probes for *VSG2*, the active *VSG* in all clones analyzed (RNAP-I), β-tubulin genes (RNAP-II), spliced-leader (SL-RNA) genes (RNAP-II), 5S rDNA genes (RNAP-III), and several negative controls: nontranscribed rDNA intergenic spacer, an insect-stage-

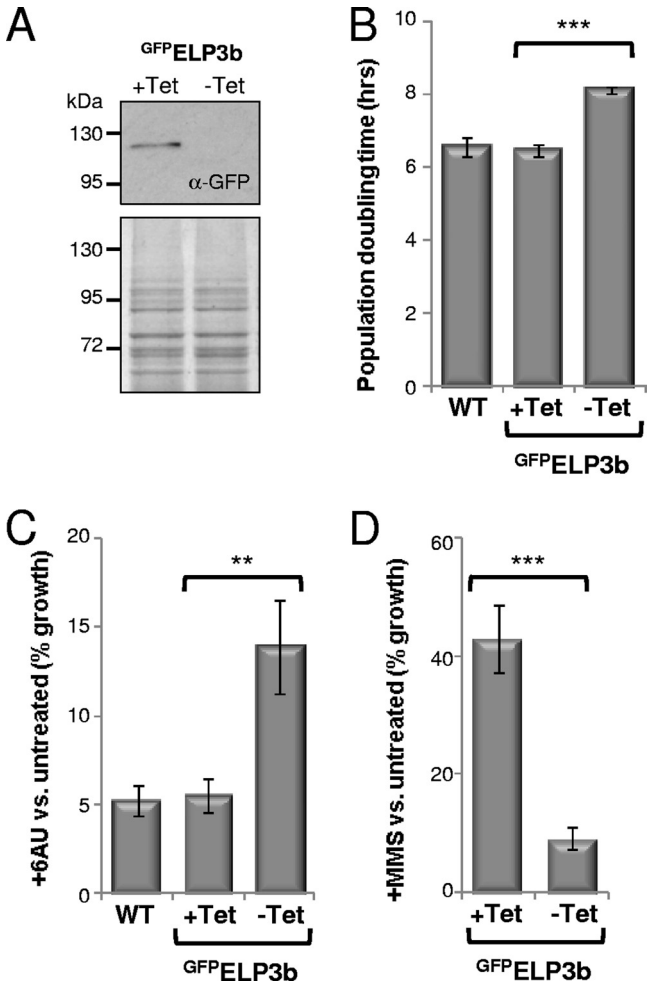

FIG. 3. ELP3 downregulation phenocopies ELP3b knockout. (A) Western blotting with anti-GFP confirmed Tet-on (1 μg ml^{-1}) regulation of ^{GFP}ELP3b in an *elp3b* background. The lower panel shows an equivalent Coomassie blue-stained gel as a loading control. Data from one representative cell line are shown. (B and C) Population doubling times (B) and 6AU (50 μg ml^{-1}) sensitivities (C) in wild-type (WT) and ^{GFP}ELP3b strains. (D) Methyl methanesulfonate (MMS; 0.0004%) sensitivity in ^{GFP}ELP3b strains (EC_{50}: +Tet, 0.00036% ± 0.000015%; −Tet, 0.00024% ± 0.000016%). The −Tet, ^{GFP}ELP3b-depleted population was assessed 4 to 7 days after Tet removal. Data in panels B to D were derived from four independent clones. Standard deviations are indicated, and *P* values were derived using a paired Student *t* test. ***, $P < 0.001$; **, $P < 0.01$.

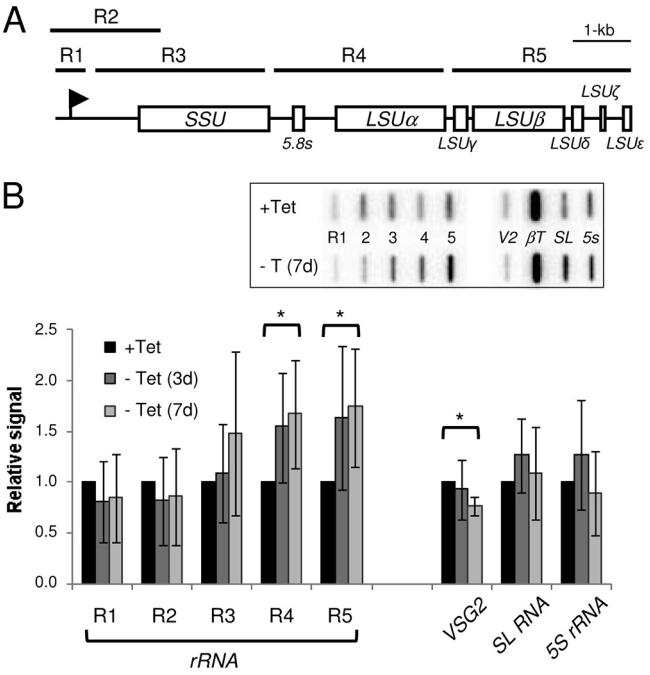

FIG. 4. ELP3b negatively regulates transcription elongation at rDNA loci. (A) Schematic of a *T. brucei* rDNA transcription unit and the location of the R1 to R5 probes (horizontal bars) for nascent transcript analysis. Each rDNA unit is approximately 10 kbp in length (55). The promoter (flag) and the rDNA subunit coding regions are indicated. (B) Transcription run-on analysis during depletion of ^{GFP}ELP3b. Phosphorimager signals were corrected against β-*tubulin* transcript abundance and expressed relative to the +Tet value (set to 1). The inset shows a sample slot blot. *V2*, *VSG2*; β*T*, β-*tubulin*. *VSG2* is a single-copy gene ~60 kbp from its promoter that is transcribed by RNAP-I. The spliced-leader RNA (SL-RNA) is derived from a tandem gene array and contributes a fragment that is *trans*-spliced to the 5′ end of every mRNA in trypanosomes. This RNA and β-*tubulin*, used as a loading control and also derived from a tandem gene array, are transcribed by RNAP-II. 5S rRNA is also derived from a tandem gene array and is transcribed by RNAP-III. Data were derived from four independent ^{GFP}ELP3b strains. Error bars represent one standard deviation, and *P* values were derived using a paired Student *t* test. *, $P < 0.05$.

specific transcript that is not expressed in the bloodstream-form cells used for this analysis (procyclin), and plasmid vector DNA. The transcription run-on analysis indicated significantly increased transcription through the rDNA unit following ^{GFP}ELP3b inactivation (Fig. 4B). In the 7-day samples, transcription was significantly increased (by >60%) across a region encompassed by probes in the middle and at the distal end of the rDNA unit (Fig. 4B). The equivalent 3-day samples also displayed increased transcription across this region but without achieving statistical significance. Probes encompassing the proximal end of the rDNA unit failed to show an increase in transcription, suggesting little attenuation in this region in wild-type cells. Thus, consistent with increased 6AU resistance, cells depleted for ELP3b displayed a relative increase in nascent rDNA promoter-distal transcripts; the large increase is remarkable given the major contribution that rDNA genes are thought to make to total transcription in unperturbed cells. Interestingly, *VSG2* transcription was significantly reduced (by ~20%) in these cells (Fig. 4B), which could reflect depletion of the extranucleolar pool of RNAP-I. No negative-control transcript, including nontranscribed rDNA intergenic spacer, was significantly above background (data not shown), and neither the RNAP-II (SL-RNA) or RNAP-III (5S rRNA) transcripts displayed significant change (Fig. 4B).

ELP3b suppresses transcription of a reporter integrated within ribosomal DNA. We next sought an independent approach to confirm negative control of transcription by ELP3b. Trypanosomes are unusual in that all mature mRNAs are fused to an RNAP-II-transcribed, *trans*-spliced leader sequence (19). This allows RNAP-I to transcribe the protein-coding segment of mRNA (45), as is the case for *VSG* genes. We took advan-

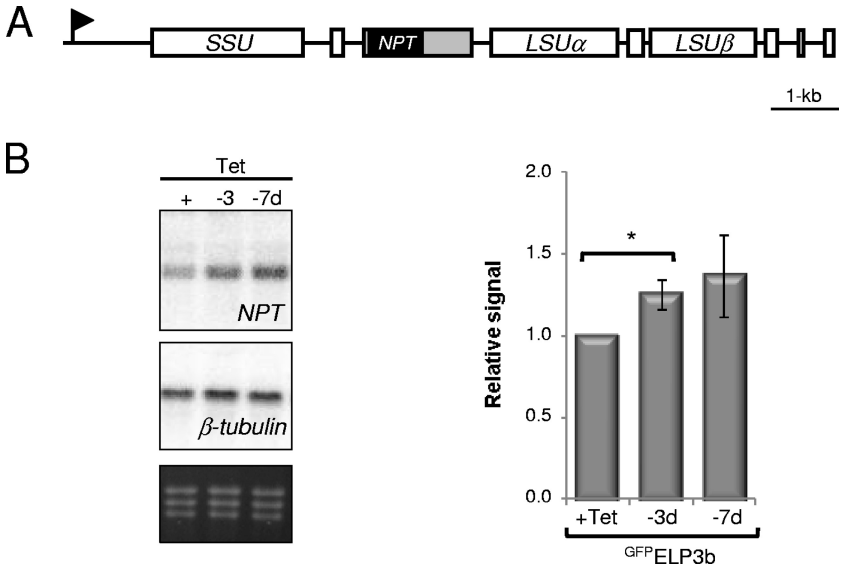

FIG. 5. ELP3b suppresses transcription of an mRNA reporter integrated at an rDNA locus. (A) Schematic of a *T. brucei* rDNA transcription unit showing the location of the neomycin phosphotransferase (*NPT*) reporter. The flanking 5′-procyclin and 3′-aldolase untranscribed regions are represented by gray boxes. (B) Northern analysis of *NPT* mRNA expression following ^{GFP}ELP3b depletion. One representative Northern blot is shown. An ethidium bromide-stained gel is included to show loading. Phosphorimager signals were processed as described for Fig. 4B. Data were derived from three independent ^{GFP}ELP3b (rDNA::*NPT*) strains. Error bars represent 1 standard deviation, and *P* values were derived using a paired Student *t* test. *, $P < 0.05$.

tage of this feature and used a selectable marker as a reporter of transcription through rDNA (Fig. 5A). A neomycin phosphotransferase (*NPT*) gene was inserted between the 5.8S and LSUα genes in cells engineered for conditional expression of ^{GFP}ELP3b in an *elp3b* null background, and three independent clones were analyzed (Fig. 5B); correct integration was confirmed using PCR assays (data not shown). *NPT* expression was increased 3 and 7 days after inactivation of ^{GFP}ELP3b expression, achieving statistical significance in the 3-day samples (Fig. 5B). The results confirm negative control of transcription through rDNA by ELP3b and suggest suppression of transcription through individual rDNA units rather than complete transcription blockade in a subset.

Having established that ELP3b negatively controls transcription at rDNA loci, we now revisited the adaptation phenomenon in the *elp3b* strains described above. We predicted that adaptation would involve reduced rDNA transcription, either through change in rDNA gene copy number or through the action of a second negative regulator. There are nine complete rDNA units annotated in the haploid *T. brucei* genome sequence, with one unit each on chromosomes 1 and 7, three on chromosome 2, and four on chromosome 3 (6). Using *elp3b* null cells grown in culture for several weeks (*elp3b**), we saw no evidence for altered rDNA gene dosage (data not shown), but as predicted, transcription run-on analysis revealed reduced rDNA transcription (Fig. 6B). In *elp3b** cells, transcription was reduced by >50% compared to the wild type in a region encompassed by three probes at the proximal end of the rDNA unit. This does not reflect more transcription in the distal region but is readily explained by a two-stage process involving increased elongation after ELP3b loss which is compensated for by less initiation (compare Fig. 6B and Fig. 4B). Consistent with adaptation in the absence of ELP3a (in *elp3a*/*elp3b* double-null strains [Fig. 2C and E]), nascent transcript analysis in *elp3a* strains did not reveal changes in rDNA transcription that were statistically significant (Fig. 6C), implicating another, unknown factor in reduced initiation and adaptation in *elp3b* null cells.

ELP3b localizes to the nucleolus but not to the *VSG* expression site body. We proceeded to explore the subcellular location of ^{GFP}ELP3a and ^{GFP}ELP3b in bloodstream-form trypanosomes engineered for tetracycline (Tet)-inducible expression (3). Microscopic analysis of these strains did not reveal any substantial GFP signal in uninduced cultures, while fluorescence or immunofluorescence analysis of induced cells indicated specific accumulation in distinct subnuclear compartments (data not shown). To directly compare these compartments, we established trypanosomes constitutively expressing both ^{GFP}ELP3a and ^{MYC}ELP3b (Fig. 7A). Immunofluorescence analysis revealed little overlap in the location of the two proteins; the subnuclear compartment occupied by ^{GFP}ELP3a is punctate and typically at the nuclear periphery, while ^{MYC}ELP3b occupies a more central compartment (Fig. 7B). We obtained similar results using insect-stage, procyclic trypanosomes (data not shown). Interestingly, the accumulation of ^{MYC}ELP3b was specifically disrupted after transcription inhibition (Fig. 7B), which could indicate engagement with active transcription factors.

Diploid *T. brucei* nuclei contain a single nucleolus, the site of rDNA transcription driven by RNAP-I, and apparent ELP3b accumulation at this site is consistent with the phenotypes described above. However, bloodstream-form *T. brucei* trypanosomes are unusual in that they also use RNAP-I to transcribe *VSG* mRNA at an extranucleolar site known as the expression site body (ESB) (32). To examine ELP3b localization with respect to both RNAP-I compartments, we estab-

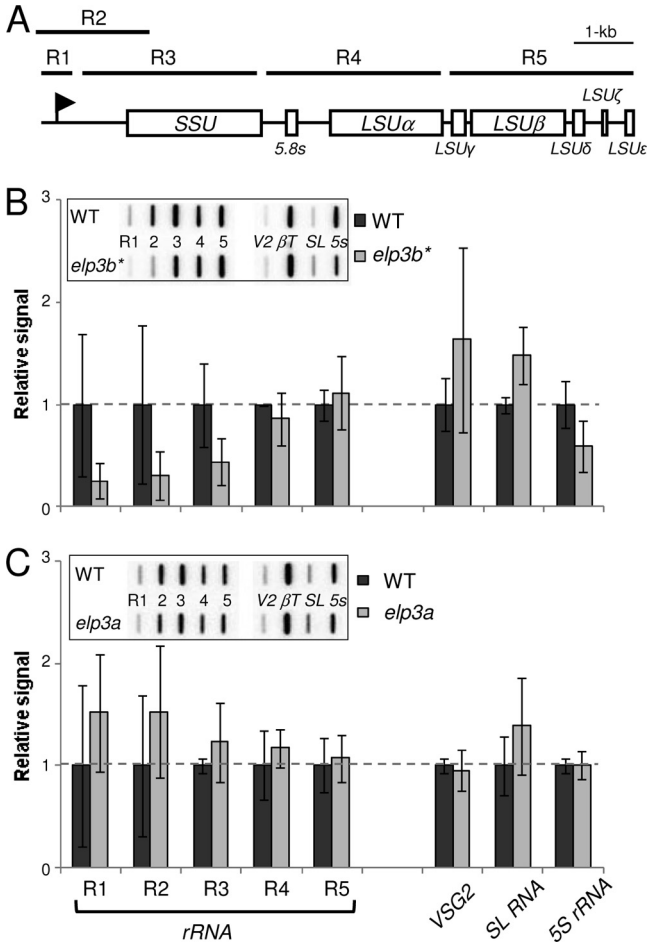

FIG. 6. Adaptation to the *elp3b* defect involves downregulation of *rRNA* transcription. (A) Schematic of a *T. brucei* rDNA transcription unit reproduced from Fig. 4A. (B) Transcription run-on analysis of adapted *elp3b** null strains. Data were derived from two independent clones. Other details are as in Fig. 4B, except that corrected values are expressed relative to the wild type (WT). (C) Transcription run-on analysis of *elp3a* null strains. Data were derived from four independent clones. Other details are as in panel B above.

lished trypanosomes expressing ^{MYC}ELP3b and ^{GFP}RPB6z (Fig. 7A), the latter being a well-characterized RNAP-I subunit found in both RNAP-I compartments (12, 33); N-terminally tagged RPB6z was previously shown to be fully functional and does not interfere with RNAP-I activity *in vitro* (33). Immunofluorescence staining of ^{GFP}RPB6z revealed the nucleolus and the ESB as expected (Fig. 7C). Dual detection of ^{GFP}RPB6z and ^{MYC}ELP3b revealed a strong ^{MYC}ELP3b signal at the nucleolus, but no detectable ^{MYC}ELP3b signal that coincided with the smaller ESB, the compartment involved in *VSG* transcription (Fig. 7C).

The data above indicated nucleolar sequestration of ELP3b and little or no association with the ESB. However, we detected some nuclei with a second compartment of ^{MYC}ELP3b staining, and we speculated that these represented nascent nucleoli. This was confirmed using cells expressing ^{GFP}ELP3b (Fig. 3A). Dual immunofluorescence detection of ^{GFP}ELP3b and NOG1, a nucleolar G protein (38) that is not detected in the ESB, indicated that the second focus of ^{GFP}ELP3b staining always colocalized with NOG1 (Fig. 7D). In addition, nuclear and mitochondrial (kinetoplast) DNAs, stained with DAPI (4′,6-diamidino-2-phenylindole), provide excellent cytological markers that define the position in the cell cycle (58), and as expected, two nucleoli and two ^{GFP}ELP3b foci in a single nucleus were observed in trypanosomes only in the G_2/M phases. Thus, ELP3b was sequestered in the nucleolus and showed little or no association with the ESB regardless of whether the protein was fused to GFP or a MYC epitope. The results show that nucleolus-enriched ^{GFP}ELP3b complemented the growth, 6AU resistance, and transcription phenotypes seen in *elp3b* cells (see above). We also demonstrated that *elp3b* cells were indistinguishable from the wild type in relation to ELP3a, NOG1, and RPB6z localization (data not shown).

We used a similar approach to further examine the compartment(s) occupied by the other Elp3-related protein, ELP3a. ^{GFP}ELP3a was coexpressed with other tagged transcription factors, and expression of proteins of the predicted size was confirmed by Western blotting (Fig. 8A). ELP3a appeared to occupy a compartment that was distinct from all three major RNA polymerases (Fig. 8B). A peripheral nuclear localization appeared more pronounced during mitosis (Fig. 8C), and partial colocalization with NUP-1, a putative nuclear lamina component (44), supported an association with the nuclear envelope (Fig. 8D). We also examined spindle microtubule acetylation, telomere position-effect repression (16), and *VSG* expression site silencing (54) in *elp3a* cells, as well as cytosine methylation (31) in *elp3a* and *elp3b* cells (data not shown), but detected no significant differences from the wild type.

ELP3b-depleted cells are hypersensitive to translation inhibition. We considered the possible benefits of limiting transcription through rDNA. This could facilitate DNA replication and DNA damage tolerance (Fig. 2F and 3D) (22) or could contribute to modulating rRNA synthesis to satisfy cellular demands for translation capacity. Indeed, rDNA transcription elongation is the rate-limiting step for rRNA synthesis in human cells (48). To explore a role for ELP3b in regulating rRNA synthesis, we examined the downstream consequences of increased rDNA transcription in ELP3b-deficient cells (Fig. 9). The trypanosomatid rDNA transcription unit is unusual in that it encodes several small rRNAs (55), but no major change in the relative steady-state abundance of any of these transcripts was seen in *elp3a*, *elp3b**, or *elp3a*/*elp3b* null cells (Fig. 9A). Furthermore, Northern blot analysis revealed no major change in relative SSU or LSU transcript abundance in ELP3b-depleted cells (Fig. 9B). To ask whether increased rDNA transcription is reflected at the level of sensitivity to translation inhibition, we assessed growth in G418. Surprisingly, ELP3b-depleted cells were hypersensitive to G418 (Fig. 9C). This was also the case in *elp3b** cells, while *elp3a* cells were indistinguishable from the wild type (data not shown). This result could reflect disruption of the ribosome assembly process, causing limiting factors to be channeled into a nonproductive pathway, or ELP3b could play an additional role in tRNA modification (21). Taken together, the results are consistent with a role for rDNA transcription control by ELP3b in maintaining genome stability rather than in modulating translation capacity.

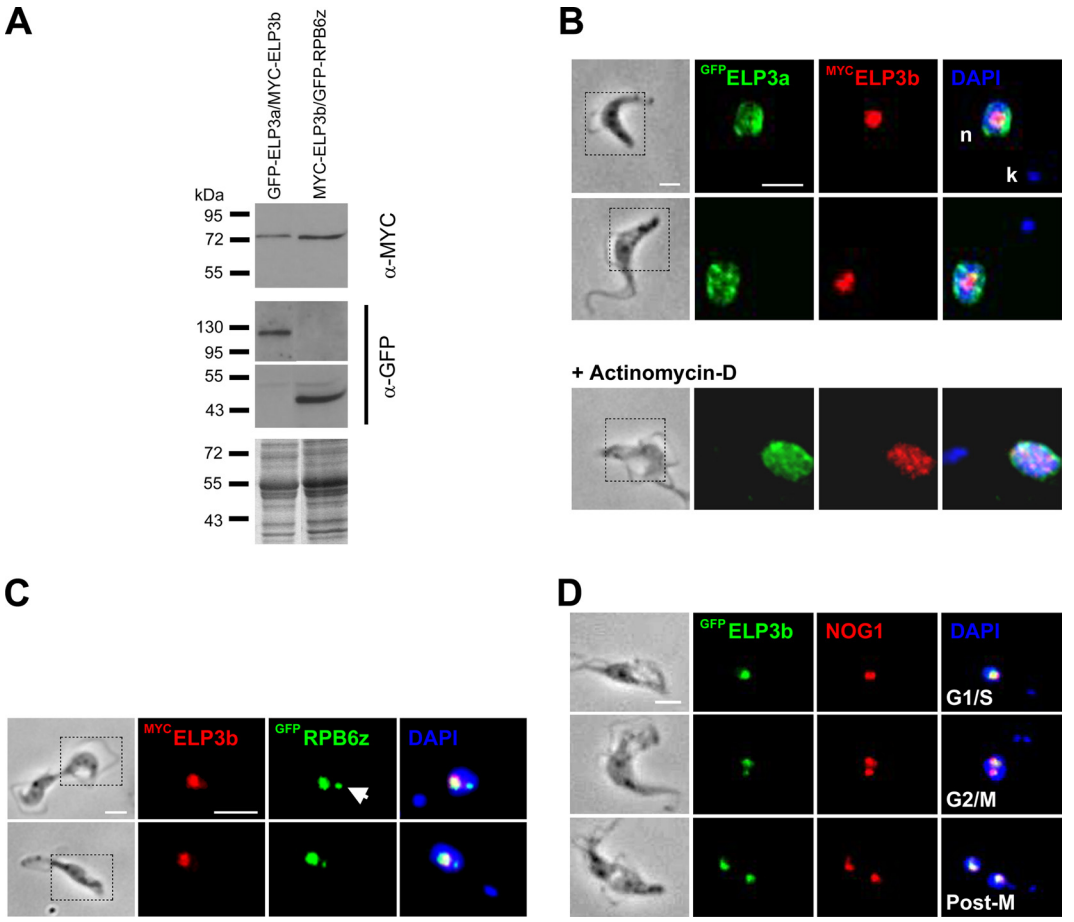

FIG. 7. ELP3b localizes to the nucleolus but is not detected in the ESB in bloodstream-form *T. brucei*. (A) Western analysis of strains used for ELP3 localization studies. Blots were incubated with anti-MYC or anti-GFP. A Coomassie blue-stained gel is included to show loading. Predicted molecular masses of the fusions: ^{GFP}ELP3a, 104 kDa; ^{MYC}ELP3b, 77 kDa; ^{GFP}RPB6z, 42 kDa. The lower anti-GFP panel is a shorter exposure. (B) Dual localization of ^{GFP}ELP3a and ^{MYC}ELP3b. The effect of actinomycin D treatment is also shown. The regions outlined in the phase images indicate the regions shown in the immunofluorescence panels. The nucleus (n) and kinetoplast (k) were stained with the DNA intercalating dye 4′,6-diamidino-2-phenylindole (DAPI), and these images were merged with the immunofluorescence images. Bar, 5 μm. (C) ^{MYC}ELP3b localizes specifically to the nucleolus but not to the smaller ESB (arrowhead), as revealed by ^{GFP}RPB6z. (D) Colocalization of ^{GFP}ELP3b and the nucleolar protein, NOG1, through the cell cycle. G_1/S cells have a single nucleolus, while a second nucleolus can be seen during G_2/M (identified by two kinetoplasts). Postmitotic (Post-M) cells have a single nucleolus in each nucleus. Other details are as in panel B above.

DISCUSSION

rDNA genes encode the core components of the ribosomes, the molecular machines that drive mRNA translation into protein. Sixty to 80 percent of transcription in rapidly growing yeast cells is at rDNA loci mediated by RNAP-I. The elongation rate has been estimated to be ~60 nucleotides/s with a reinitiation rate of <1 s (14). Despite the important link to genome stability (22), the balance between silencing and activating complexes and their contributions to the formation of alternative chromatin states at these loci remain poorly understood (30). A number of factors that typically control multiple classes of RNA polymerase have been shown to exert positive (7, 59) and negative (30) control on RNAP-I elongation at rDNA genes. In addition, structural analysis reveals that *S. cerevisiae* RNAP-I contains a built-in elongation factor related to the RNAP-II-associated factor TFIIF (27), and a mutated phosphorylation site on *S. cerevisiae* RNAP-I increases resistance to 6AU, consistent with a role in negative control of elongation (15). We have demonstrated negative control by ELP3b that is specific to nucleolar rDNA genes in trypanosomes, and our reporter analysis suggests suppression of individual rDNA transcription units rather than complete blockade of a subset.

Nucleosomes are depleted or disordered at actively transcribed rDNA loci (30). Thus, ELP3b may generate a more stable or "closed" chromatin state that promotes premature termination. How might this be achieved? rDNA gene regulation involves histone modification and DNA methylation (50), and ELP3b, like other Elp3 orthologues, has two major domains, an acetyltransferase domain and a radical SAM domain. Histone acetylation is important for transcription initiation and elongation, and a specific enrichment of histone H4K10 acetylation, H2AZ and H2BV histone variants, and the BDF3 bromodomain factor is seen at probable RNAP-II transcription start sites in trypanosomes (47). These same variants are depleted within the nontranscribed rDNA spacer, and

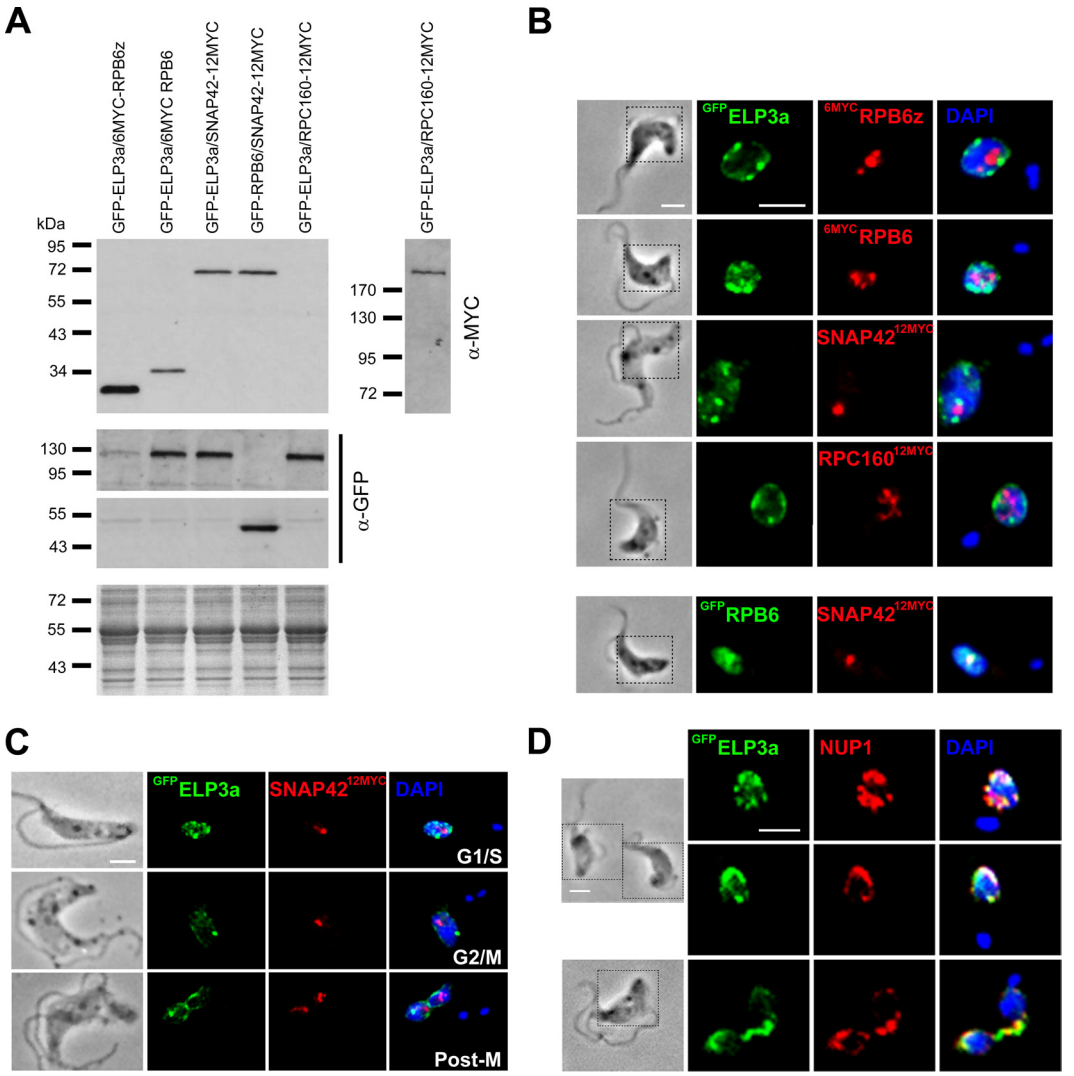

FIG. 8. ELP3a occupies nuclear territories distinct from those occupied by the transcription machinery. (A) Western analysis of strains used for ELP3 localization studies. Predicted molecular masses of the fusions: ^{6MYC}RPB6z, 24 kDa; ^{6MYC}RPB6, 25 kDa; ^{GFP}RPB6, 43 kDa; SNAP42^{12MYC}, 60 kDa; RPC160^{12MYC}, 188 kDa. (B) ^{GFP}ELP3a and the tagged polymerase subunits occupy distinct nuclear territories. ^{6MYC}RPB6z, RNAP-I; ^{6MYC}RPB6 and SNAP42^{12MYC}, RNAP-II (colocalization of these factors is associated with sites of SL-RNA transcription [30, 52]); RPC160^{12MYC}, RNAP-III. (C) Localization of ^{GFP}ELP3a and SNAP42^{12MYC} through the cell cycle. (D) ^{GFP}ELP3a shows partial colocalization with NUP1. Other details are as in Fig. 7B.

BDF3 is depleted in the transcribed rDNA region, revealing a distinct chromatin architecture at these loci (see the region encompassing Tb927.3.3421 to Tb927.3.3455 at http://tritrypdb.org/). Importantly, histone acetylation has also been associated with negative control of transcription (9, 24, 29, 53). Thus, acetylation by ELP3b may negatively control rDNA transcription elongation. The radical SAM domain could equally be responsible for negative control, possibly via DNA demethylation (36).

The nucleus is highly heterogeneous, containing euchromatic and heterochromatic compartments thought to be permissive and repressive for transcription, respectively. RNAP-I transcribes rDNA genes in the nucleolar compartment, and, in *T. brucei*, RNAP-I also synthesizes a subset of abundant pre-mRNAs. In fact, *T. brucei* is the only known eukaryote with a multifunctional RNAP-I and presents a unique opportunity to study RNAP-I regulators. The trypanosomatid RNAP-I complex (34, 52) contains three "specialized" subunits, RPB5z, RPB6z, and RPB10z (12), as well as RPA31 (33) and the RPB7 subunit, typically associated with RNAP-II (39). Trypanosome RNAP-I transcription also depends upon a novel complex known as class I transcription factor A (8). ELP3b has not been identified in fractions containing *T. brucei* RNAP-I (8, 33, 34, 52), possibly due to weak or little direct interaction or because the majority of RNAP-I is engaged in processive transcription. Remarkably though, ELP3b specifically impacts relatively short RNAP-I transcription units (rDNA, 10 kbp) and appears to be excluded from a much longer RNAP-I transcription unit at the ESB (*VSG*, 60 kbp). Several additional nucleolar factors are undetectable in the ESB, but ELP3b is the first of these factors shown to distinguish between rDNA and *VSG* mRNA synthesis. The distinct promoters that operate at these loci could determine this differential association.

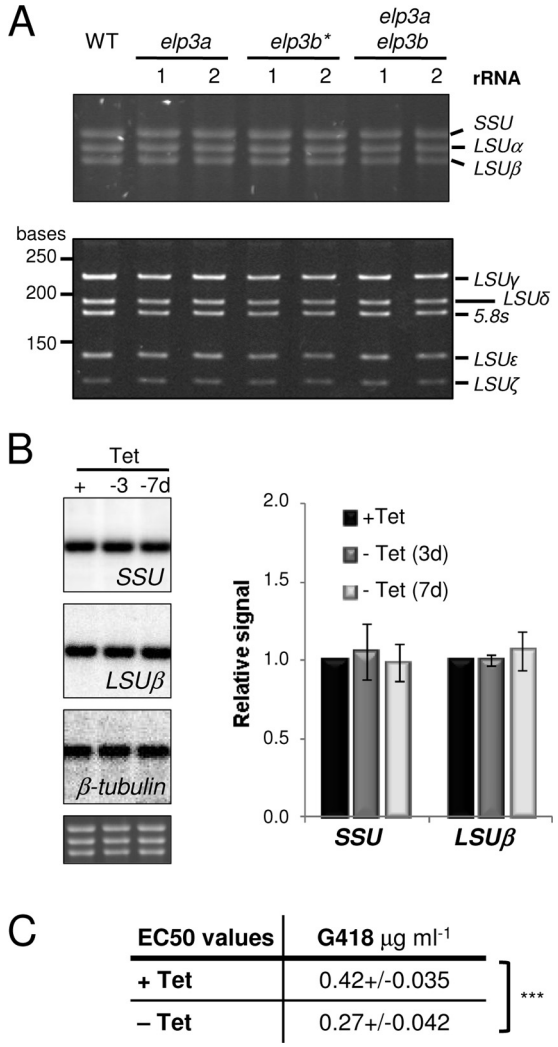

C

EC50 values	G418 μg ml^{-1}	
+ Tet	0.42+/-0.035	***
– Tet	0.27+/-0.042	

FIG. 9. ELP3b loss is associated with hypersensitivity to translation inhibition. (A) Total RNA from the wild type and pairs of *elp3a*, *elp3b*, and *elp3a*/*elp3b* null strains was fractionated by agarose-formaldehyde (upper panel) or polyacrylamide-urea (lower panel) gel electrophoresis. (B) Northern analysis of steady-state rRNA transcripts following depletion of ^{GFP}ELP3b. One representative blot is shown. An ethidium bromide-stained gel is included to show loading. Phosphorimager signals were processed as described for Fig. 4B. Data were derived from four independent ^{GFP}ELP3b strains. (C) EC_{50} values for G418 and ^{GFP}ELP3b strains, + and −Tet. −Tet cultures were maintained in Tet-free medium for 3 days prior to G418 treatment. Data were derived from four independent ^{GFP}ELP3b strains. Standard deviations are indicated, and *P* values were derived using a paired Student *t* test. ***, $P < 0.001$.

Microarray analysis of steady-state transcripts in Elongator-defective *S. cerevisiae* revealed 52 genes that were downregulated and 44 genes that were upregulated (26). Under the conditions examined here, ELP3b negatively controls rDNA transcription and can be considered an "anti-Elongator." We suggest that this may also be the case at the upregulated loci in *S. cerevisiae*. Indeed, Elp3 was recently shown to have a role in maintaining silencing at telomeres and at mating-type loci in *S. cerevisiae* (28). Our results indicate a negative role for ELP3b in processivity, while, at this stage, the role of ELP3a remains unknown.

The purpose of limited transcription through rDNA appears to be to improve genome stability (22). Our results are consistent with the idea that unregulated transcription of rDNA genes is indeed toxic and compromises the capacity for DNA repair at these loci. Our findings could reflect a conserved role for Elp3 proteins in this process. Indeed, Elp3 is concentrated in nucleoli in HeLa cells (20). We favor a model whereby ELP3b, like Elp3 in *S. cerevisiae*, associates with elongating RNAP and modifies chromatin structure, but we cannot rule out other possible scenarios to explain negative control of RNAP-I processivity at this stage. Targeted meganuclease cleavage (17) could now be used to further explore the impact of ELP3b transcription control on double-strand break repair within rDNA transcription units. It will also be important to determine what contributions the ELP3b acetyltransferase and radical SAM domains make to the novel anti-Elongator function described here.

ACKNOWLEDGMENTS

This work was supported by The Wellcome Trust (project grants 079457 and 083648).

We also thank John Kelly (LSHTM) for critical reading of the manuscript, Marilyn Parsons (Seattle Biomedical Research Institute) for NOG1 antisera, Klaus Ersfeld (University of Hull, United Kingdom) for NUP1 antisera, and Elisabetta Ullu (Yale University) for the transcription run-on protocol.

REFERENCES

1. **Alibu, V. P., L. Storm, S. Haile, C. Clayton, and D. Horn.** 2005. A doubly inducible system for RNA interference and rapid RNAi plasmid construction in *Trypanosoma brucei*. Mol. Biochem. Parasitol. **139:**75–82.
2. **Alsford, S., and D. Horn.** 2008. Single-locus targeting constructs for reliable regulated RNAi and transgene expression in *Trypanosoma brucei*. Mol. Biochem. Parasitol. **161:**76–79.
3. **Alsford, S., T. Kawahara, L. Glover, and D. Horn.** 2005. Tagging a *T. brucei RRNA* locus improves stable transfection efficiency and circumvents inducible expression position effects. Mol. Biochem. Parasitol. **144:**142–148.
4. **Alsford, S., T. Kawahara, C. Isamah, and D. Horn.** 2007. A sirtuin in the African trypanosome is involved in both DNA repair and telomeric gene silencing but is not required for antigenic variation. Mol. Microbiol. **63:**724–736.
5. **Ausubel, F. M., et al.** 1998. Current protocols in molecular biology. John Wiley and Sons, Inc., New York, NY.
6. **Berriman, M., et al.** 2005. The genome of the African trypanosome *Trypanosoma brucei*. Science **309:**416–422.
7. **Birch, J. L., et al.** 2009. FACT facilitates chromatin transcription by RNA polymerases I and III. EMBO J. **28:**854–865.
8. **Brandenburg, J., et al.** 2007. Multifunctional class I transcription in *Trypanosoma brucei* depends on a novel protein complex. EMBO J. **26:**4856–4866.
9. **Braunstein, M., R. E. Sobel, C. D. Allis, B. M. Turner, and J. R. Broach.** 1996. Efficient transcriptional silencing in *Saccharomyces cerevisiae* requires a heterochromatin histone acetylation pattern. Mol. Cell. Biol. **16:**4349–4356.
10. **Clayton, C. E.** 2002. Life without transcriptional control? From fly to man and back again. EMBO J. **21:**1881–1888.
11. **Creppe, C., et al.** 2009. Elongator controls the migration and differentiation of cortical neurons through acetylation of α-tubulin. Cell **136:**551–564.
12. **Devaux, S., et al.** 2007. Diversification of function by different isoforms of conventionally shared RNA polymerase subunits. Mol. Biol. Cell **18:**1293–1301.
13. **Figueiredo, L. M., G. A. Cross, and C. J. Janzen.** 2009. Epigenetic regulation in African trypanosomes: a new kid on the block. Nat. Rev. Microbiol. **7:**504–513.
14. **French, S. L., Y. N. Osheim, F. Cioci, M. Nomura, and A. L. Beyer.** 2003. In exponentially growing *Saccharomyces cerevisiae* cells, rRNA synthesis is determined by the summed RNA polymerase I loading rate rather than by the number of active genes. Mol. Cell. Biol. **23:**1558–1568.
15. **Gerber, J., et al.** 2008. Site specific phosphorylation of yeast RNA polymerase I. Nucleic Acids Res. **36:**793–802.
16. **Glover, L., and D. Horn.** 2006. Repression of polymerase I-mediated gene expression at *Trypanosoma brucei* telomeres. EMBO Rep. **7:**93–99.

17. **Glover, L., R. McCulloch, and D. Horn.** 2008. Sequence homology and microhomology dominate chromosomal double-strand break repair in African trypanosomes. Nucleic Acids Res. **36:**2608–2618.
18. **Guenther, M. G., S. S. Levine, L. A. Boyer, R. Jaenisch, and R. A. Young.** 2007. A chromatin landmark and transcription initiation at most promoters in human cells. Cell **130:**77–88.
19. **Gunzl, A.** 2010. The pre-mRNA splicing machinery of trypanosomes: complex or simplified? Eukaryot. Cell **9:**1159–1170.
20. **Hawkes, N. A., et al.** 2002. Purification and characterization of the human elongator complex. J. Biol. Chem. **277:**3047–3052.
21. **Huang, B., M. J. Johansson, and A. S. Bystrom.** 2005. An early step in wobble uridine tRNA modification requires the Elongator complex. RNA **11:**424–436.
22. **Ide, S., T. Miyazaki, H. Maki, and T. Kobayashi.** 2010. Abundance of ribosomal RNA gene copies maintains genome integrity. Science **327:**693–696.
23. **Ivens, A. C., et al.** 2005. The genome of the kinetoplastid parasite, *Leishmania major*. Science **309:**436–442.
24. **Kawahara, T., et al.** 2008. Two essential MYST-family proteins display distinct roles in histone H4K10 acetylation and telomeric silencing in trypanosomes. Mol. Microbiol. **69:**1054–1068.
25. **Kim, J. H., W. S. Lane, and D. Reinberg.** 2002. Human Elongator facilitates RNA polymerase II transcription through chromatin. Proc. Natl. Acad. Sci. U. S. A. **99:**1241–1246.
26. **Krogan, N. J., and J. F. Greenblatt.** 2001. Characterization of a six-subunit holo-elongator complex required for the regulated expression of a group of genes in *Saccharomyces cerevisiae*. Mol. Cell. Biol. **21:**8203–8212.
27. **Kuhn, C. D., et al.** 2007. Functional architecture of RNA polymerase I. Cell **131:**1260–1272.
28. **Li, Q., et al.** 2009. The elongator complex interacts with PCNA and modulates transcriptional silencing and sensitivity to DNA damage agents. PLoS Genet. **5:**e1000684.
29. **Liang, G., et al.** 2004. Distinct localization of histone H3 acetylation and H3-K4 methylation to the transcription start sites in the human genome. Proc. Natl. Acad. Sci. U. S. A. **101:**7357–7362.
30. **McStay, B., and I. Grummt.** 2008. The epigenetics of rRNA genes: from molecular to chromosome biology. Annu. Rev. Cell Dev. Biol. **24:**131–157.
31. **Militello, K. T., et al.** 2008. African trypanosomes contain 5-methylcytosine in nuclear DNA. Eukaryot. Cell **7:**2012–2016.
32. **Navarro, M., and K. Gull.** 2001. A pol I transcriptional body associated with *VSG* mono-allelic expression in *Trypanosoma brucei*. Nature **414:**759–763.
33. **Nguyen, T. N., B. Schimanski, and A. Gunzl.** 2007. Active RNA polymerase I of *Trypanosoma brucei* harbors a novel subunit essential for transcription. Mol. Cell. Biol. **27:**6254–6263.
34. **Nguyen, T. N., B. Schimanski, A. Zahn, B. Klumpp, and A. Gunzl.** 2006. Purification of an eight subunit RNA polymerase I complex in *Trypanosoma brucei*. Mol. Biochem. Parasitol. **149:**27–37.
35. **Ogbadoyi, E., K. Ersfeld, D. Robinson, T. Sherwin, and K. Gull.** 2000. Architecture of the *Trypanosoma brucei* nucleus during interphase and mitosis. Chromosoma **108:**501–513.
36. **Okada, Y., K. Yamagata, K. Hong, T. Wakayama, and Y. Zhang.** 2010. A role for the elongator complex in zygotic paternal genome demethylation. Nature **463:**554–558.
37. **Otero, G., et al.** 1999. Elongator, a multisubunit component of a novel RNA polymerase II holoenzyme for transcriptional elongation. Mol. Cell **3:**109–118.
38. **Park, J. H., B. C. Jensen, C. T. Kifer, and M. Parsons.** 2001. A novel nucleolar G-protein conserved in eukaryotes. J. Cell Sci. **114:**173–185.
39. **Penate, X., et al.** 2009. RNA pol II subunit RPB7 is required for RNA pol I-mediated transcription in *Trypanosoma brucei*. EMBO Rep. **10:**252–257.
40. **Pokholok, D. K., N. M. Hannett, and R. A. Young.** 2002. Exchange of RNA polymerase II initiation and elongation factors during gene expression *in vivo*. Mol. Cell **9:**799–809.
41. **Rahl, P. B., C. Z. Chen, and R. N. Collins.** 2005. Elp1p, the yeast homolog of the FD disease syndrome protein, negatively regulates exocytosis independently of transcriptional elongation. Mol. Cell **17:**841–853.
42. **Raz, B., M. Iten, Y. Grether-Buhler, R. Kaminsky, and R. Brun.** 1997. The Alamar Blue assay to determine drug sensitivity of African trypanosomes (*T.b. rhodesiense* and *T.b. gambiense*) *in vitro*. Acta Trop. **68:**139–147.
43. **Roberts, J. W., S. Shankar, and J. J. Filter.** 2008. RNA polymerase elongation factors. Annu. Rev. Microbiol. **62:**211–233.
44. **Rout, M. P., and M. C. Field.** 2001. Isolation and characterization of subnuclear compartments from *Trypanosoma brucei*. Identification of a major repetitive nuclear lamina component. J. Biol. Chem. **276:**38261–38271.
45. **Rudenko, G., H. M. Chung, V. P. Pham, and L. H. Van der Ploeg.** 1991. RNA polymerase I can mediate expression of CAT and neo protein-coding genes in *Trypanosoma brucei*. EMBO J. **10:**3387–3397.
46. **Shaw, R. J., and D. Reines.** 2000. *Saccharomyces cerevisiae* transcription elongation mutants are defective in *PUR5* induction in response to nucleotide depletion. Mol. Cell. Biol. **20:**7427–7437.
47. **Siegel, T. N., et al.** 2009. Four histone variants mark the boundaries of polycistronic transcription units in *Trypanosoma brucei*. Genes Dev. **23:**1063–1076.
48. **Stefanovsky, V., F. Langlois, T. Gagnon-Kugler, L. I. Rothblum, and T. Moss.** 2006. Growth factor signaling regulates elongation of RNA polymerase I transcription in mammals via UBF phosphorylation and r-chromatin remodeling. Mol. Cell **21:**629–639.
49. **Svejstrup, J. Q.** 2007. Elongator complex: how many roles does it play? Curr. Opin. Cell Biol. **19:**331–336.
50. **Tucker, S., A. Vitins, and C. S. Pikaard.** 2010. Nucleolar dominance and ribosomal RNA gene silencing. Curr. Opin. Cell Biol. **22:**351–356.
51. **Ullu, E., and C. Tschudi.** 1990. Permeable trypanosome cells as a model system for transcription and trans-splicing. Nucleic Acids Res. **18:**3319–3326.
52. **Walgraffe, D., et al.** 2005. Characterization of subunits of the RNA polymerase I complex in *Trypanosoma brucei*. Mol. Biochem. Parasitol. **139:**249–260.
53. **Wang, A., S. K. Kurdistani, and M. Grunstein.** 2002. Requirement of Hos2 histone deacetylase for gene activity in yeast. Science **298:**1412–1414.
54. **Wang, Q. P., T. Kawahara, and D. Horn.** 2010. Histone deacetylases play distinct roles in telomeric *VSG* expression site silencing in African trypanosomes. Mol. Microbiol. **77:**1237–1245.
55. **White, T. C., G. Rudenko, and P. Borst.** 1986. Three small RNAs within the 10 kb trypanosome *rRNA* transcription unit are analogous to domain VII of other eukaryotic 28S rRNAs. Nucleic Acids Res. **14:**9471–9489.
56. **Winkler, G. S., A. Kristjuhan, H. Erdjument-Bromage, P. Tempst, and J. Q. Svejstrup.** 2002. Elongator is a histone H3 and H4 acetyltransferase important for normal histone acetylation levels *in vivo*. Proc. Natl. Acad. Sci. U. S. A. **99:**3517–3522.
57. **Wittschieben, B. O., et al.** 1999. A novel histone acetyltransferase is an integral subunit of elongating RNA polymerase II holoenzyme. Mol. Cell **4:**123–128.
58. **Woodward, R., and K. Gull.** 1990. Timing of nuclear and kinetoplast DNA replication and early morphological events in the cell cycle of *Trypanosoma brucei*. J. Cell Sci. **95:**49–57.
59. **Zhang, Y., M. L. Sikes, A. L. Beyer, and D. A. Schneider.** 2009. The Paf1 complex is required for efficient transcription elongation by RNA polymerase I. Proc. Natl. Acad. Sci. U. S. A. **106:**2153–2158.